Title

Kinetochore kinesin CENP-E is a processive bi-directional tracker of dynamic microtubule tips.

Journal

Nature cell biology, 15(9)

ISSN

1465-7392

Authors

Gudimchuk, Nikita
Vitre, Benjamin
Kim, Yumi
et al.

Publication Date

2013-09-01

DOI

10.1038/ncb2831

Peer reviewed

HHS Public Access

Author manuscript

Nat Cell Biol. Author manuscript; available in PMC 2014 March 01.

Published in final edited form as:

Nat Cell Biol. 2013 September ; 15(9): 1079–1088. doi:10.1038/ncb2831.

Kinetochore kinesin CENP-E is a processive bi-directional tracker of dynamic microtubule tips

Nikita Gudimchuk[#1], **Benjamin Vitre**[#2], **Yumi Kim**[2,†], **Anatoly Kiyatkin**[1], **Don W. Cleveland**[2], **Fazly I. Ataullakhanov**[3,4], and **Ekaterina L. Grishchuk**[1,#]

[1]Physiology Department, Perelman School of Medicine, University of Pennsylvania, Philadelphia, PA, United States

[2]Ludwig Institute for Cancer Research and Department of Cellular and Molecular Medicine, Univ. of California, San Diego, La Jolla, CA, United States

[3]Center for Theoretical Problems of Physicochemical Pharmacology, Russian Academy of Sciences, Moscow, Russian Federation

[4]Federal Research and Clinical Centre of Pediatric Hematology, Oncology and Immunology, Moscow, Russian Federation

[#] These authors contributed equally to this work.

Abstract

During vertebrate mitosis, the centromere-associated kinesin CENP-E transports misaligned chromosomes to the plus ends of spindle microtubules. Subsequently, the kinetochores that form at the centromeres establish stable associations with microtubule ends, which assemble and disassemble dynamically. Here we provide evidence that after chromosomes have congressed and bi-oriented, the CENP-E motor continues to play an active role at kinetochores, enhancing their links with dynamic microtubule ends. Using a combination of single molecule approaches and laser trapping in vitro we demonstrate that once reaching microtubule ends, CENP-E converts from a lateral transporter into a microtubule tip-tracker which maintains association with both assembling and disassembling microtubule tips. Computational modeling of this behavior supports our proposal that CENP-E tip-tracks bi-directionally via a “tethered motor” mechanism, which relies on both the motor and tail domains of CENP-E. Our results provide a molecular framework for CENP-E's contribution to the stability of attachments between kinetochores and dynamic microtubule ends.

[#]Correspondence to: gekate@mail.med.upenn.edu.

[†]Current address: Department of Molecular and Cell Biology, University of California, Berkeley, CA, United States

Author contributions: N.G. performed in vitro experiments and mathematical modeling; B.V. and A.K. performed in vivo experiments; B.V. and Y.K. purified proteins; N.G., B.V., F.I.A., D.W.C. and E.L.G. designed research, analyzed data and wrote the paper.

Competing financial interests: The authors declare no competing financial interests.

INTRODUCTION

Accurate chromosome segregation depends on interactions between microtubules (MTs) and kinetochore, a protein structure localized at each centromere[1]. Initially, kinetochores often attach to the walls of MTs with the chromosomes then moving toward a spindle pole in a dynein-dependent manner[2,3]. The pole-proximal chromosomes then need to congress, i.e. move to the spindle midzone where MT plus ends are located. The centromere protein CENP-E, a MT-dependent plus-end directed motor of the kinesin-7 subfamily, is essential for congression of initially misaligned chromosomes[4–8]. Perturbation of CENP-E function using antibody injection[9] or depletion[10], gene inactivation[11], siRNA depletion[12], or inhibition with a small molecule inhibitor[13] blocks MT plus-end-directed motion of pole-proximal chromosomes, accompanied by a failure of both kinetochores to form stable MT attachments[11].

Previous work has suggested that the role of CENP-E in mitosis is not limited to the transport of chromosomes during congression. First, CENP-E is detected at the kinetochores of already congressed chromosomes[14,15]. Second, depletion of CENP-E induces up to a 50% reduction in the number of MTs on congressed chromosomes[11,16]. Third, CENP-E gene deletion leads to an increased proportion of lagging chromosomes in anaphase in mouse liver cells and embryonic fibroblasts[11,17]. Fourth, after CENP-E-mediated congression, CENP-E-dependent localization of protein phosphatase 1 (PP1) to kinetochores is still required for stable microtubule capture by those kinetochores[8]. Furthermore, antibodies to CENP-E block the motions of isolated mammalian chromosomes at the ends of depolymerizing MTs in vitro[18]. Despite these observations, whether CENP-E plays a physiological role at the kinetochore-MT interface of congressed chromosomes and the possible underlying molecular mechanisms for these findings remain controversial.

Mechanochemical enzymes like kinesins transport intracellular cargos by walking along MT tracks. The well-studied kinesin-1, a plus-end-directed motor, carries axonal organelles towards MT ends, where the motor dissociates from the MT and unloads its cargo[19]. However, the chromosomal cargo carried by CENP-E kinesin is unusual; after the kinetochore has encountered the ends of the MT tracks, it does not detach but remains stably associated with the tips of MTs[20,21]. The nature of the connections that link the kinetochores of congressed chromosomes and MT ends is not well understood, but these links are known to permit exchange of tubulin dimers at the MT ends, implying that each kinetochore can processively track dynamic MT ends[20,22]. This is a remarkable property because the kinetochore maintains its attachment to the site where tubulin dimers are being added or lost on the MT polymer. Only two proteins that exhibit bi-directional tip-tacking in vitro have thus been identified[23–25]. Here we examine whether the CENP-E kinesin can facilitate such end-on MT attachments.

RESULTS

The CENP-E motor acts at kinetochores of congressed chromosomes

To investigate a possible contribution of CENP-E to linking MT plus ends to the kinetochores on congressed chromosomes we used a specific small molecule inhibitor

GSK-923295, which locks CENP-E in a "rigor" MT-bound state[13]. HeLa cells were arrested in metaphase with a proteasome inhibitor, which was then replaced with the CENP-E inhibitor or DMSO as a control (Fig. 1a). In control metaphase cells CENP-E was clearly visible at the kinetochores (Fig. 1b); chromosome alignment was maintained in all but 1 out of 50 cells and anaphase started ~30 min after removing the proteasome inhibitor (Fig.1c, d). Addition of GSK-923295 to metaphase cells caused a marked depletion of the kinetochore-localized CENP-E (Fig. 1e), probably due to the passive transport of the rigor bound motor by poleward MT flux[6]. Importantly, in ~50% of CENP-E-inhibited cells there was a clear loss of chromosome alignment (3.6 chromosome pairs per cell). One of the sister kinetochores on such pairs appeared to assume MT-lateral binding, and moved toward the pole (Fig. 1e, lower inset). Subsequently, these chromosomes accumulated at the poles and anaphase was delayed (Video S1), the hallmark features of the loss of CENP-E function[9,11,17]. These results clearly demonstrate that CENP-E contributes not only to the congression of pole-proximal chromosomes[5,7], but it also continues to be motor active at the kinetochores of congressed chromosomes.

Single molecules of full length and truncated CENP-E walk similarly along MT walls

The above finding prompted us to reconstitute CENP-E interactions with MTs in vitro using purified proteins. To examine transport properties of the previously uncharacterized wild type version of CENP-E, thereafter called full length (FL) CENP-E, we used total internal reflection fluorescence (TIRF) microscopy to visualize a C-terminal fusion of it to GFP (Fig. 2a,b). Many encounters between single FL molecules and coverslip-attached, Taxol-stabilized MTs led to short-lived diffusive motions, suggesting auto-inhibition of soluble FL CENP-E[26,27] (Fig. 2c, S1a-d). However, some FL molecules in our preparations lacked such inhibition and moved unidirectionally and processively, similar to a truncated (TR) CENP-E, in which the motor domains were dimerized with a shortened coiled-coil stalk[6,28] (Fig. 2a). These proteins were then conjugated by their C-termini to 0.5μm beads, and laser tweezers were used to launch these beads on MT walls (Figs. S1e-g, Video S2). A significantly larger fraction of processive motions was observed with beads coated with FL CENP-E vs. what was seen with the soluble bead-free molecules (Fig. S1h), suggesting that conjugating the tail of FL CENP-E to a bead cargo partially relieves the auto-inhibition, as in kinesin-1[29]. Detailed quantification of the single molecule and bead motility in these assays revealed that the MT wall-dependent transport by FL motor is highly similar to that of TR CENP-E (Table S1)[8,28,30].

Single molecules of FL but not TR CENP-E can processively track dynamic MT ends

We then analyzed what happens when CENP-E walks to the ends of MT tracks. Upon reaching the plus tips of stable MTs, both FL and TR CENP-E constructs paused at the tip for 2-4 sec before detaching[8], significantly longer than 0.3±0.1sec (Mean±SEM, n=253) for kinesin-1 studied under identical conditions (Fig. S2a and Table S2). This finding may explain an increase in the rate of MT polymerization, which was observed previously with human truncated CENP-E motor in the presence of Taxol[31]. To examine how CENP-E interacts with the physiologically relevant, dynamic MT ends, we grew non-stabilized polymers from coverslip-attached MT seeds (Fig. 3a). Both FL and TR CENP-E proteins walked fast enough to catch up with the growing MT end. Interestingly, the TR molecules

detached from these ends more rapidly than from the tips of Taxol-stabilized MTs (Figs. 3b, S2; Video S3). However, a large fraction of FL CENP-E molecules did not dissociate from the polymerizing ends and continued to move with MT elongation, which was 15 times slower than the motor's walking rate (Figs. 3c,d, S3). This marked slowing is unlikely to result from the different nucleotide composition of the growing tip vs. MT wall because FL CENP-E moved only slightly slower on the GMPCPP vs. GDP-containing lattices (Fig. S3c). A slower motility on GMPCPP-containing segments was also observed for TR CENP-E, yet it failed to track processively with the polymerizing tip (Fig. S2c).

About 70% of FL motors that walked into a disassembling MT tip also did not dissociate but moved backwards in the direction opposite to the motor-dependent motility, while following the rapidly disassembling MT (Fig. 3d; Videos S4, S5). By quantifying GFP intensity of the tip-tracking complexes we found that many contained only 2 GFP molecules and therefore were dimers of CENP-E (Figs. 3e, S3 e-g). The tip-tracking complexes sometimes appeared to diffuse near the tip. This behavior was more evident at polymerizing tips, presumably because polymerization is 10-times slower than depolymerization (Figs. 3d, Video S6). FL CENP-E dimers remained associated with growing and shortening tips for 17.9±1.3 and 11.6±1.4 sec, respectively, resulting in the travel lengths of 0.3±0.1 and 2.1±0.3 μm (Fig. S4a-d; Table S2). Small teams of FL molecules tracked even better, sometimes remaining at the tip for several rounds of MT growth and shortening (Video S7). These brighter complexes tended to slow MT depolymerization (Fig. S3b), but single tip-tracking dimers did not affect significantly either the rates of growth and shortening, or catastrophe frequency (Fig. 3f). Thus, CENP-E has a capacity to track processively with both assembling and disassembling MTs at a single molecule level, a property not shared by previously studied kinesins.

CENP-E can couple MT disassembly to bead motion in vitro

CENP-E has been observed to localize to the plus ends of spindle MTs in human cells, consistent with its tip-tracking in vivo[15]. Furthermore, prior work implicated CENP-E in assisting motions of isolated mammalian chromosomes at the ends of depolymerizing MTs in vitro[18]. To test directly whether purified FL CENP-E can couple MT dynamics to cargo motion, we used segmented MTs, an in vitro approach we previously developed to study MT depolymerization-dependent motions[32] (Fig. 4a). With laser tweezers, CENP-E-coated beads were brought to the walls of MTs, transiently stabilized by caps made from GMPCPP-containing Rhodamine-labeled tubulin. These beads walked toward the capped plus-ends, mimicking chromosomal transport during congression. When MT depolymerization was triggered by photo-ablating the stabilizing caps, almost all FL CENP-E-coated beads followed the shortening MT ends (Fig. 3b-e), demonstrating the ability of CENP-E to couple beads motions with MT disassembly. Such coupling required the non-motor domains of CENP-E as TR CENP-E-coated beads failed to track (Videos S8, S9).

CENP-E contributes to stable association between depolymerizing MT ends and kinetochores

To test a possible role for CENP-E in linking kinetochores and dynamic MT ends, we designed an experiment to trigger chromosome transport by depolymerizing MTs in vivo[33]

(Fig. 5a). Monopolar spindles were induced in HeLa cells that expressed the kinetochore marker Mis12-GFP. After chromosomes assumed their positions at the plus tips of astral MTs, the CENP-E motor was inhibited with GSK-923295, after which MT depolymerization was triggered by nocodazole (Fig. 5b). Live imaging of control cells with no CENP-E inhibitor revealed that nocodazole-induced MT shortening produced chromosome motion toward the unseparated poles (Figs. 5c,d). Inhibiting CENP-E, however, greatly reduced the ability of chromosomes to move in conjunction with MT disassembly (Video S10).

To rule out that the CENP-E inhibitor directly affected the MT stability, cells were subjected to the same treatments (as in Fig. 5b), but their spindles were visualized with tubulin-EYFP. MT depolymerization commenced in <1 min in all cells treated with nocodazole, but adding GSK-923295 alone had no effect (Fig. S5). No gross changes in MT asters were seen in cells that were fixed and immunostained 25 min after adding GSK-923295, as judged by spindle tubulin intensity (Fig. S6). The diameters of MT asters were slightly larger in GSK-923295 treated cells, further indicating that this inhibitor did not induce MT disassembly (Fig. S6c). Next, cells were pretreated with GSK-923295 for 5 min to deplete CENP-E from the kinetochores, then additionally treated with nocodazole and cold to promote MT disassembly. In ~60% of these cells some chromosomes were left at the periphery with no attached cold-stable MT fibers (Figs. 5e,f; S7a). This is a significantly larger fraction than when nocodazole was used with no CENP-E inhibitor, consistent with live imaging results. Furthermore, the GSK-923295 pretreated cells had fewer tubulin-containing MT remnants than the cells with CENP-E-depleted kinetochores (Fig. S6a,d). Similar results were also seen when CENP-E was disrupted by RNAi in another human cell line and similar experiments were done without GSK-923295 (Figs. 5g,h; S7b). We conclude that presence of CENP-E motor at the kinetochores promotes their ability to maintain stable connections with disassembling MT ends.

Tip-tracking of CENP-E is not caused by its high affinity to MT tips, but requires its motor and C-terminal tail

To dissect the molecular mechanisms underlying the processive tip-tracking we tested two specific hypotheses. First, we asked if tip-tracking could result from the increased affinity of CENP-E to MT tips vs. walls. With a fluorescence-based MT-pelleting assay we measured CENP-E binding to GDP- and GMPCPP-containing MTs, mimicking the growing MT tips: the apparent dissociation constants were 41±4 nM and 68±23 nM, respectively (Fig. 6a). Binding affinity to the depolymerizing MT tips, as measured with tubulin spirals that are similar in structure to the curved tubulin protofilaments[34], was 133±22 nM. Thus, CENP-E shows no significant preference to the tip-mimicking structures, suggesting that its bi-directional tip-tracking is unlikely to results from different affinities.

Since TR CENP-E was unable to track MT ends processively, we next investigated if the C-terminal tail of CENP-E was involved (Fig. 2a). FL bound stronger to Taxol-stabilized MTs than the TR protein (144±54 nM; Fig. 6a), consistent with the presence of a MT-binding site in its tail[26,35]. We expressed and purified a C-terminal CENP-E fragment fused with GFP (Tail, Fig. 6b). This fragment lies distally to the kinetochore-targeting sequence of CENP-

E[26,36], so the tails of kinetochore-bound CENP-E molecules may be positioned to interact directly with kinetochore MTs in vivo. Purified Tail molecules bound and diffused rapidly on MTs but failed to follow the dynamic tips, indicating that tail was not the sole determinant of the bi-directional tip-tracking (Fig. 6c-f). Interestingly, statistical analysis of motions of the Tail at the dynamic MT ends has revealed that only 1 out of 10 encounters between the Tail and dynamic MT end resulted in Tail's detachment (see Materials and Methods), with the majority of Tail molecules bouncing back from the tip and continuing to diffuse along the MT wall, as if “reflected” by the tip (Fig. 6 g,h).

A “tethered motor” mechanism provides a quantitative fit for bi-directional MT tip-tracking by CENP-E

Based on the above results we then hypothesized that even though neither the tail nor the motor domain could track the dynamic MT ends on their own, a combination of their molecular properties produced a collective tip-tracking behavior. We tested this hypothesis in a mechanistic and quantitative way with a mathematical model based on the detailed kinetic schemes (Figs. 7a,b). The model describes molecular interactions between the MT wall, tip, and the motor and tail domains connected together via a worm-like tether (see Supplementary Note for detail description of model assumptions and Table S3 for parameter values). This quantitative model recapitulated the major results of our in vitro studies with TR and FL CENP-E, including rapid dissociation of the TR motor from dynamic MT ends and the ability of FL CENP-E to tip-track processively (Figs. 7c-f). It also provided a physical mechanism for the cooperative action of motor and tail domains by demonstrating that FL CENP-E can track bi-directionally by repeating the cycles of plus end-directed walking and the tail-mediated diffusion of the MT wall-tethered motor (Videos S11, S12). The tail-MT wall association, although transient, keeps the tail-tethered motor heads in the vicinity of MT. We estimate that tethered motor heads re-associate with the wall within a millisecond, so the tail serves as a safety leash for the motor heads, which dissociate rapidly and repeatedly from the tip. Remarkably, this behavior in silico does not rely on difference(s) between assembling and disassembling ends, explaining how CENP-E tracks with both types of ends.

The proposed “tethered motor” mechanism of tip-tracking is strongly supported by our experimental observations of diffusive motions of the tip-tracking FL molecules, as evidenced by the ragged appearance of kymographs (Fig. 8 a-c). Several examples of visible excursions at both elongating and shortening MT ends are shown in Fig. S3d, and the smaller diffusive motions at the tips were common (e.g. Video S6). We challenged our model by testing experimentally its two key predictions. First, we examined tip-tracking in the presence of the non-hydrolysable ATP analog, AMPPNP, which induces strong MT-binding. Consistent with the model's prediction, the inhibited FL CENP-E failed to follow the disassembling MT tips (Fig. 8d), demonstrating that the motor's walking is required for processive tip-tracking. Second, we recapitulated the wild-type FL CENP-E motions by artificially joining the non-tracking TR CENP-E and Tail proteins. Qdots coated with the mixture of these proteins exhibited robust walking and also moved processively with both assembling and disassembling MT ends (Fig. 8e). Thus, tail and motor domains cooperate together to provide processive tip association.

DISCUSSION

Here we describe the results of the integrated study of motility of CENP-E kinesin and its physiological implications using in vivo, in vitro and in silico approaches. Experiments in two human cell lines show that kinetochore-MT attachments in disassembling monopolar spindles are greatly destabilized when CENP-E function is perturbed with either a specific inhibitor or RNAi depletion. Furthermore, we establish a continuing in vivo requirement for CENP-E motor activity at the kinetochores of congressed and bi-oriented chromosomes. Together with our discovery of CENP-E's ability to associate with the ends of dynamic MTs in vitro, these findings suggest a previously unrecognized function for this essential kinesin in accurate chromosome segregation. We propose that in addition to its established role in transporting polar chromosomes, CENP-E also facilitates the association between kinetochore and dynamic MT ends. In vitro, CENP-E kinesin can convert from a lateral transporter into a MT tip-tracker, so a similar activity may contribute to the formation of end-on MT attachments for the chromosomes that congress via a kinetochore-fiber-independent pathway[7]. Although a significant fraction of CENP-E protein leaves kinetochores after congression, CENP-E is clearly present at the kinetochores of bi-oriented chromosomes[14,15], and our results in vivo establish the physiological role of this CENP-E population in maintaining end-on MT attachments. These findings are supported by previous studies in different cells systems including Drosophila[37], mouse[11] and human cells[16], and they also provide a molecular mechanism to explain a reduced number of kinetochore MTs on congressed chromosomes in CENP-E depleted cells[11,16].

Since we have shown that a single dimer of CENP-E can maintain long-lasting association with a dynamic MT end in vitro without significantly affecting MT dynamics, we also propose that a major component of the mechanism underlying CENP-E-mediated stabilization of kinetochore-MT attachments is a direct one, provided by its ability to serve as a “mobile” molecular bond between the kinetochore and dynamic kinetochore-MT tip. Future work, however, is required to examine whether the kinetochore-bound CENP-E can also affect dynamics of kinetochore MTs, since multiple CENP-E molecules may act in concert at kinetochores. Furthermore, in the context of live cells the tip-tracking by CENP-E may promote kinetochore-MT attachment not only directly but also in conjunction with additional activities from other associated proteins, such as CLASP1/2[38,39] or PP1 phosphatase[8].

Our work also provides a detailed molecular mechanism to explain how CENP-E can track MT tips processively and bi-directionally. The autonomous tip-tracking that we have uncovered for CENP-E is distinct from that of proteins like EB1. Despite being widely referred to as a plus-tip-tracking protein, the individual molecules of EB1 do not associate continuously with growing MTs and tip-tracking is not processive[40]. Only two proteins, XMAP215[23] and Dam1 oligomers[25,41,42], neither with motor activity, have previously been described to track dynamic MT tips processively and bi-directionally at a single molecule level. Members of the kinesin-8 family, the plus-end-directed Kif18A and Kip3, can associate processively with the growing MT tip in vitro, assisted by their C-terminal tails[43–46]. These motors, however, fail to track disassembling MTs. The molecular mechanism of their unidirectional plus-end-tracking is not known, so it may include the

affinity-based interactions specifically at the assembling tips. Alternatively, kinesin-8 may tip-track with the growing MTs by the mechanism we propose here for CENP-E. Our computational model provides insight into protein's ability to tip-track uni- vs. bi-directionally by emphasizing a complex interrelationship between the rates of protein diffusion and MT dynamics[47]. The reported diffusion of the Kif18A tail is 100-times slower than that of the CENP-E tail[43,45]. In silico, motors with both tails can travel with the elongating MT end quite well because both tails diffuse rapidly relative to the slow rate of MT assembly (Fig. 8f). However, the slowly diffusing tail is predicted to dissociate sooner from the shortening MT ends because MT disassembly is rapid enough to catch up repeatedly with the molecule that diffuses slowly “in front” of the wave of tubulin depolymerization. Each of these encounters may cause a stochastic loss of the terminal tubulin dimer together with the bound tail molecule, so the slower diffusing Kif18A tail is not a good tether for the shortening MT end. It remains to be seen if the “tethered motor” mechanism that we propose is employed by other MT-dependent motors, or this specialization is unique to kinetochore-localized kinesin-7.

Supplementary Material

Refer to Web version on PubMed Central for supplementary material.

Acknowledgments

We thank members of Grishchuk and Ataullakhanov labs for stimulating discussions and technical assistance, A. Korbalev for help with the model videos, M. Porter for a kind gift of axonemes, M. Ostap, M. Lampson and J.R. McIntosh for critical reading of the manuscript, E. Ballister and M. Lampson for assistance with live cell imaging. We thank University of California, San Diego, Neuroscience Microscopy Shared Facility (P30 NS047101), and J.R. McIntosh for help with the initial phase of this work (GM 033787). This work has been supported by grants from the NIH to E.L.G. (R01-GM098389) and to D.W.C. (R01-GM29513), and grants to F.I.A from Russian Fund for Basic Research (12-04-00111-a) and Presidium of Russian Academy of Sciences (Mechanisms of the Molecular Systems Integration and Molecular and Cell Biology programs). B.V. has been supported by a postdoctoral fellowship from the Human Frontiers Science Program. E.L.G. is a Kimmel Scholar; her work is supported in part by the Pennsylvania Muscle Institute. D.W.C. receives salary support from the Ludwig Institute for Cancer Research.

Abbreviations

D-tip	depolymerizing microtubule tip
FL	full length CENP-E
MT	microtubule
TIRF	total internal reflection fluorescence
TR	truncated CENP-E
P-tip	polymerizing microtubule tip

References

1. Cleveland DW, Mao Y, Sullivan KF. Centromeres and kinetochores: from epigenetics to mitotic checkpoint signaling. Cell. 2003; 112:407–421. [PubMed: 12600307]

2. Rieder CL, Alexander SP. Kinetochores are transported poleward along a single astral microtubule during chromosome attachment to the spindle in newt lung cells. J. Cell Biol. 1990; 110:81–95. [PubMed: 2295685]
3. Yang Z, Tulu US, Wadsworth P, Rieder CL. Kinetochore dynein is required for chromosome motion and congression independent of the spindle checkpoint. Curr. Biol. 2007; 17:973–980. [PubMed: 17509882]
4. Yen TJ, et al. CENP-E, a novel human centromere-associated protein required for progression from metaphase to anaphase. EMBO J. 1991; 10:1245–1254. [PubMed: 2022189]
5. Kapoor TM, et al. Chromosomes Can Congress to the Metaphase Plate Before Biorientation. Science. 2006; 311:388–391. [PubMed: 16424343]
6. Kim Y, Heuser JE, Waterman CM, Cleveland DW. CENP-E combines a slow, processive motor and a flexible coiled coil to produce an essential motile kinetochore tether. J Cell Biol. 2008; 181:411–419. [PubMed: 18443223]
7. Cai S, O'Connell CB, Khodjakov A, Walczak CE. Chromosome congression in the absence of kinetochore fibres. Nat. Cell Biol. 2009; 11:832–838. [PubMed: 19525938]
8. Kim Y, Holland AJ, Lan W, Cleveland DW. Aurora kinases and protein phosphatase 1 mediate chromosome congression through regulation of CENP-E. Cell. 2010; 142:444–455. [PubMed: 20691903]
9. Schaar BT, Chan GK, Maddox P, Salmon ED, Yen TJ. CENP-E function at kinetochores is essential for chromosome alignment. J. Cell Biol. 1997; 139:1373–1382. [PubMed: 9396744]
10. Wood KW, Sakowicz R, Goldstein LS, Cleveland DW. CENP-E is a plus end-directed kinetochore motor required for metaphase chromosome alignment. Cell. 1997; 91:357–366. [PubMed: 9363944]
11. Putkey FR, et al. Unstable kinetochore-microtubule capture and chromosomal instability following deletion of CENP-E. Dev. Cell. 2002; 3:351–365. [PubMed: 12361599]
12. Yao X, Abrieu A, Zheng Y, Sullivan KF, Cleveland DW. CENP-E forms a link between attachment of spindle microtubules to kinetochores and the mitotic checkpoint. Nat. Cell Biol. 2000; 2:484–491. [PubMed: 10934468]
13. Wood KW, et al. Antitumor activity of an allosteric inhibitor of centromere-associated protein-E. Proc. Natl. Acad. Sci. U.S.A. 2010; 107:5839–5844. [PubMed: 20167803]
14. Brown KD, Wood KW, Cleveland DW. The kinesin-like protein CENP-E is kinetochore-associated throughout poleward chromosome segregation during anaphase-A. J Cell Sci. 1996; 109:961–969. [PubMed: 8743943]
15. Cooke CA, Schaar B, Yen TJ, Earnshaw WC. Localization of CENP-E in the fibrous corona and outer plate of mammalian kinetochores from prometaphase through anaphase. Chromosoma. 1997; 106:446–455. [PubMed: 9391217]
16. McEwen BF, et al. CENP-E is essential for reliable bioriented spindle attachment, but chromosome alignment can be achieved via redundant mechanisms in mammalian cells. Mol. Biol. Cell. 2001; 12:2776–2789. [PubMed: 11553716]
17. Weaver BAA, et al. Centromere-associated protein-E is essential for the mammalian mitotic checkpoint to prevent aneuploidy due to single chromosome loss. J. Cell Biol. 2003; 162:551–563. [PubMed: 12925705]
18. Lombillo VA, Nislow C, Yen TJ, Gelfand VI, McIntosh JR. Antibodies to the kinesin motor domain and CENP-E inhibit microtubule depolymerization-dependent motion of chromosomes in vitro. J. Cell Biol. 1995; 128:107–115. [PubMed: 7822408]
19. Hirokawa N, Noda Y, Tanaka Y, Niwa S. Kinesin superfamily motor proteins and intracellular transport. Nature Reviews Molecular Cell Biology. 2009; 10:682–696. [PubMed: 19773780]
20. McIntosh JR, Grishchuk EL, West RR. Chromosome-Microtubule Interactions During Mitosis. Annual Review of Cell and Developmental Biology. 2002; 18:193–219.
21. Walczak CE, Cai S, Khodjakov A. Mechanisms of chromosome behaviour during mitosis. Nat. Rev. Mol. Cell Biol. 2010; 11:91–102. [PubMed: 20068571]
22. Rieder CL, Salmon E. The vertebrate cell kinetochore and its roles during mitosis. Trends in Cell Biology. 1998; 8:310–318. [PubMed: 9704407]

23. Brouhard GJ, et al. XMAP215 is a processive microtubule polymerase. Cell. 2008; 132:79–88. [PubMed: 18191222]
24. Westermann S, et al. The Dam1 kinetochore ring complex moves processively on depolymerizing microtubule ends. Nature. 2006; 440:565–569. [PubMed: 16415853]
25. Lampert F, Hornung P, Westermann S. The Dam1 complex confers microtubule plus end-tracking activity to the Ndc80 kinetochore complex. J. Cell Biol. 2010; 189:641–649. [PubMed: 20479465]
26. Espeut J, et al. Phosphorylation relieves autoinhibition of the kinetochore motor Cenp-E. Mol. Cell. 2008; 29:637–643. [PubMed: 18342609]
27. Lu H, Ali MY, Bookwalter CS, Warshaw DM, Trybus KM. Diffusive movement of processive kinesin-1 on microtubules. Traffic. 2009; 10:1429–1438. [PubMed: 19682327]
28. Yardimci H, van Duffelen M, Mao Y, Rosenfeld SS, Selvin PR. The mitotic kinesin CENP-E is a processive transport motor. Proc. Natl. Acad. Sci. U.S.A. 2008; 105:6016–6021. [PubMed: 18427114]
29. Coy DL, Hancock WO, Wagenbach M, Howard J. Kinesin's tail domain is an inhibitory regulator of the motor domain. Nat. Cell Biol. 1999; 1:288–292. [PubMed: 10559941]
30. Shastry S, Hancock WO. Interhead tension determines processivity across diverse N-terminal kinesins. Proc. Natl. Acad. Sci. U.S.A. 2011; 108:16253–16258. [PubMed: 21911401]
31. Sardar HS, Luczak VG, Lopez MM, Lister BC, Gilbert SP. Mitotic kinesin CENP-E promotes microtubule plus-end elongation. Curr. Biol. 2010; 20:1648–1653. [PubMed: 20797864]
32. Grishchuk EL, Molodtsov MI, Ataullakhanov FI, McIntosh JR. Force production by disassembling microtubules. Nature. 2005; 438:384–388. [PubMed: 16292315]
33. Inoue S. The effect of colchicine on the microscopic and submicroscopic structure of the mitotic spindle. Exp. Cell Res. 1952; 2(Suppl.):305–318.
34. Marantz R, Shelanski ML. Structure of microtubular crystals induced by vinblastine in vitro. J. Cell Biol. 1970; 44:234–238. [PubMed: 5409462]
35. Liao H, Li G, Yen TJ. Mitotic regulation of microtubule cross-linking activity of CENP-E kinetochore protein. Science. 1994; 265:394–398. [PubMed: 8023161]
36. Chan GK, Schaar BT, Yen TJ. Characterization of the kinetochore binding domain of CENP-E reveals interactions with the kinetochore proteins CENP-F and hBUBR1. J. Cell Biol. 1998; 143:49–63. [PubMed: 9763420]
37. Yucel JK, et al. CENP-meta, an essential kinetochore kinesin required for the maintenance of metaphase chromosome alignment in Drosophila. J. Cell Biol. 2000; 150:1–11. [PubMed: 10893249]
38. Maffini S, et al. Motor-independent targeting of CLASPs to kinetochores by CENP-E promotes microtubule turnover and poleward flux. Curr. Biol. 2009; 19:1566–1572. [PubMed: 19733075]
39. Maia ARR, et al. Cdk1 and Plk1 mediate a CLASP2 phospho-switch that stabilizes kinetochore microtubule attachments. The Journal of Cell Biology. 2012; 199:285–301. [PubMed: 23045552]
40. Dixit R, et al. Microtubule plus-end tracking by CLIP-170 requires EB1. Proc. Natl. Acad. Sci. U.S.A. 2009; 106:492–497. [PubMed: 19126680]
41. Gestaut DR, et al. Phosphoregulation and depolymerization-driven movement of the Dam1 complex do not require ring formation. Nat. Cell Biol. 2008; 10:407–414. [PubMed: 18364702]
42. Grishchuk EL, et al. Different assemblies of the DAM1 complex follow shortening microtubules by distinct mechanisms. Proc. Natl. Acad. Sci. U.S.A. 2008; 105:6918–6923. [PubMed: 18460602]
43. Stumpff J, et al. A tethering mechanism controls the processivity and kinetochore-microtubule plus- end enrichment of the kinesin-8 Kif18A. Mol. Cell. 2011; 43:764–775. [PubMed: 21884977]
44. Su X, et al. Mechanisms underlying the dual-mode regulation of microtubule dynamics by Kip3/kinesin-8. Mol Cell. 2011; 43:751–763. [PubMed: 21884976]
45. Mayr MI, Storch M, Howard J, Mayer TU. A non-motor microtubule binding site is essential for the high processivity and mitotic function of kinesin-8 Kif18A. PLoS ONE. 2011; 6:e27471. [PubMed: 22102900]
46. Weaver LN, et al. Kif18A uses a microtubule binding site in the tail for plus-end localization and spindle length regulation. Curr. Biol. 2011; 21:1500–1506. [PubMed: 21885282]

47. Grishchuk, EL.; McIntosh, JR.; Molodtsov, MI.; Ataullakhanov, FI. Comprehensive Biophysics. Vol. 4. Elsevier B.V; 2012. p. 93-117.

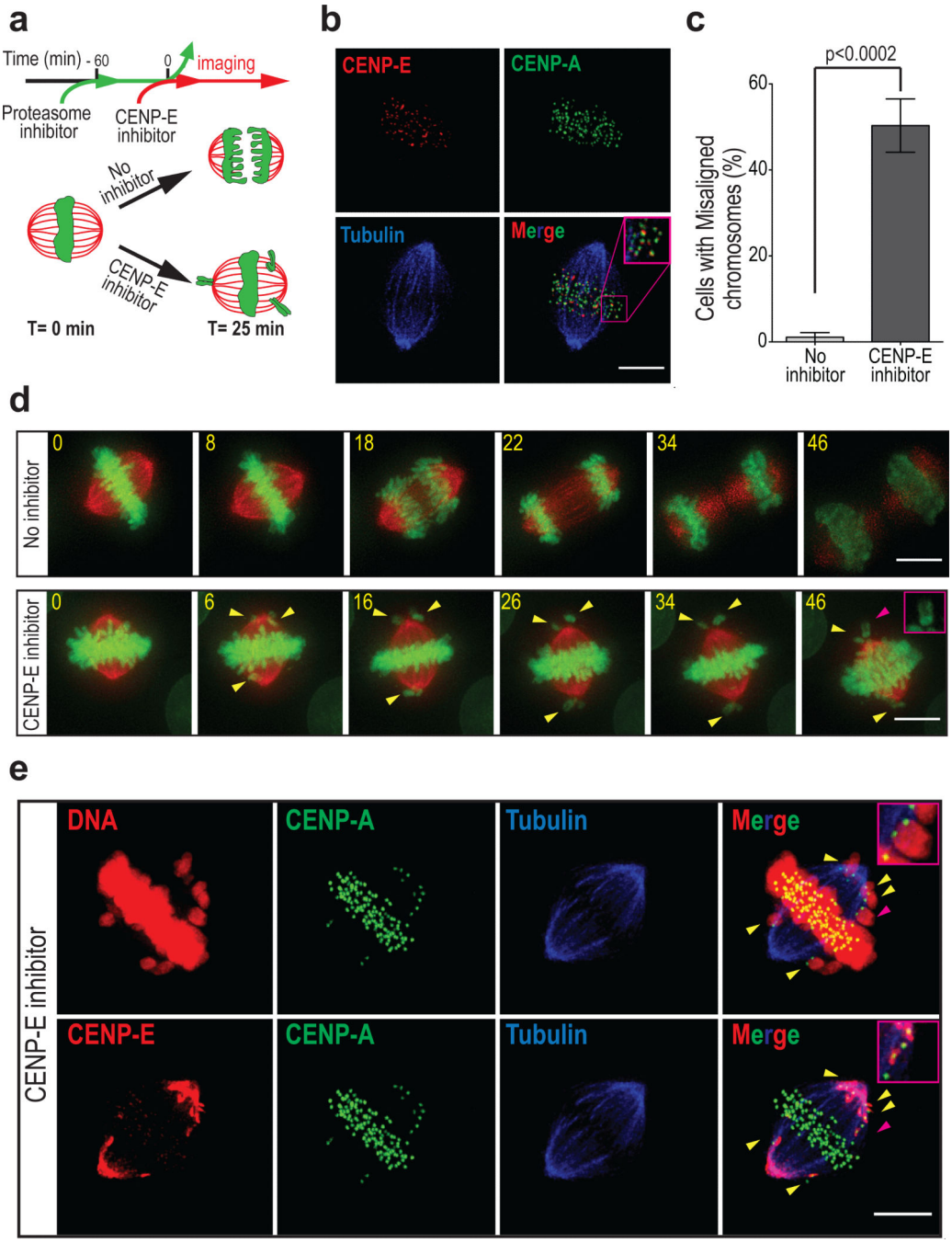

Figure 1. Loss of chromosome alignment in metaphase cells with inhibited CENP-E kinesin

(a) Schematics of the assay with metaphase-arrested HeLa cells. **(b)** Immunostaining of a HeLa cell arrested at metaphase with the proteasome inhibitor Velcade, CENP-A is a centromere/kinetochore marker. **(c)** Percent of cells in which at least one chromosome lost its alignment (Mean ± SEM); based on n=3 independent experiments (50 cells total) for "no inhibitor" condition and n=4 independent experiments (70 cells total) for "CENP-E inhibitor" condition. Two-tailed unpaired t test indicates significant differences between these results. **(d)** Time-lapse images of HeLa cells treated with Velcade for 1 hour, then

released into medium containing DMSO or GSK-923295 (Video S1). Numbers are minutes after Velcade washout. Arrows point to chromosomes that lost alignment (yellow) or that are enlarged in the inset (pink). **(e)** Immunofluorescence images of a HeLa cell released from Velcade into CENP-E inhibitor for 15 min and stained for DNA, CENP-A, CENP-E and tubulin; 3 color overlays are shown in each row. Scale bars: 5 μm.

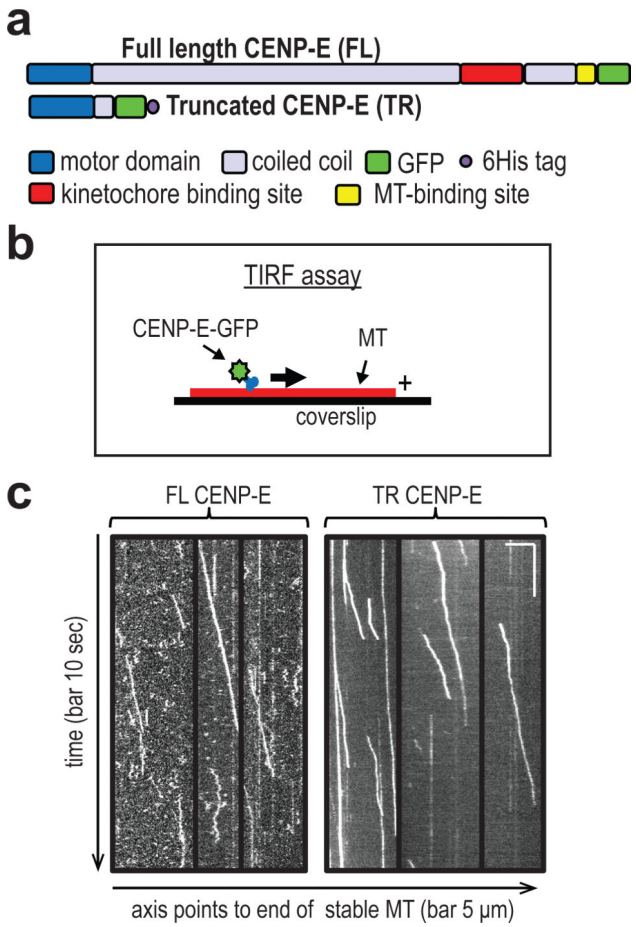

Figure 2. Motility of single molecules of CENP-E on MT wall

(a) Domain structure of the *Xenopus laevis* CENP-E proteins used for in vitro experiments. These drawings are not to scale; FL CENP-E is almost 230 nm long[6], but both proteins have C-terminal GFP fusions. **(b)** Schematics of the TIRF assay with stable MTs. **(c)** Typical kymographs of single molecule motions. Fewer FL CENP-E molecules show processive plus-end-directed walking but these motions are quantitatively similar to the walking of TR CENP-E motor.

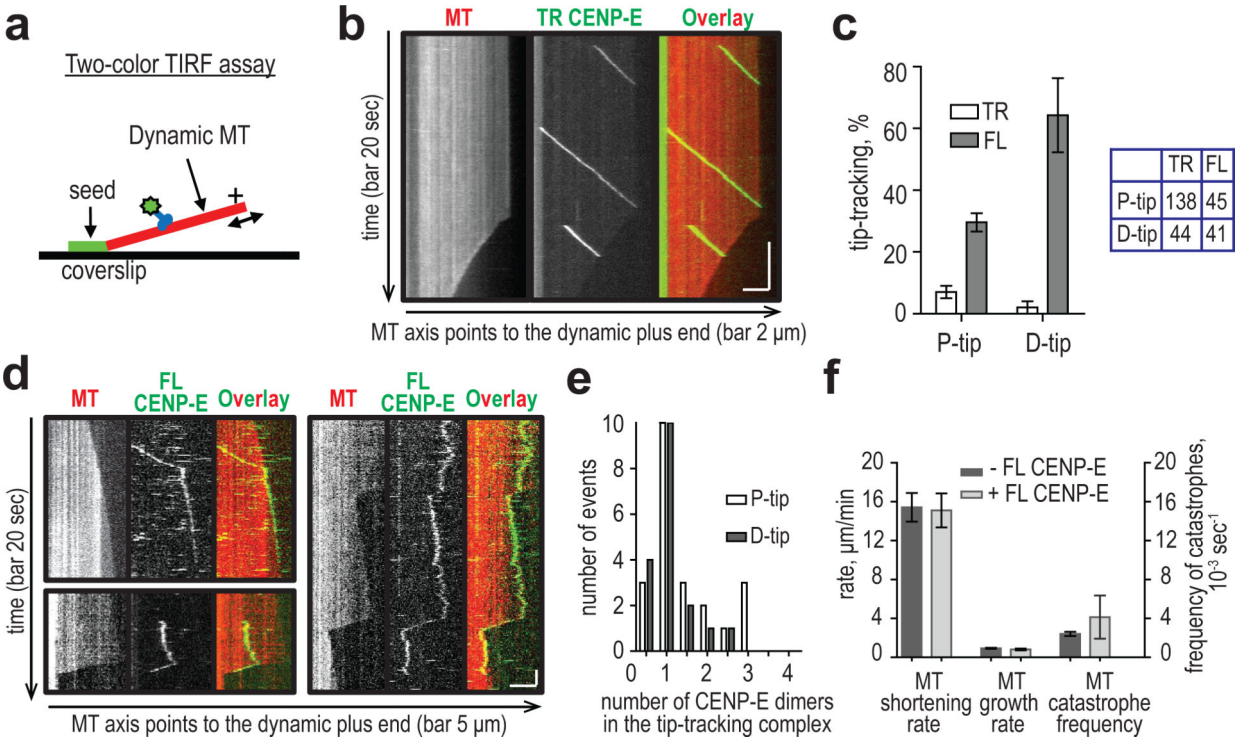

Figure 3. Single molecules of CENP-E visualized at dynamic MT tips

(a) Schematics of single molecule assay with dynamic MTs. **(b)** Kymographs of walking TR CENP-E molecules, which fall off the growing, then shrinking MT tip. (**c**) Percent of complexes tracking the polymerizing (P-tip) and depolymerizing (D-tip) MT from the total number of molecules that reached MT end (Mean ± SEM). n=8 independents experiments for FL CENP-E. Two experiments with TR CENP-E were analyzed by bootstrap analysis with n=1,000 samples. Complexes that were observed at the end of dynamic MT for at least 4 sec were called “tip-tracking”. Table shows number of complexes analyzed for each group. **(d)** Kymographs of FL CENP-E tracking the tip of the growing (upper left panel) and shortening (bottom left panel) MTs. Right panel shows continuous motion with the end of one dynamic MT. **(e)** Histogram of the number of CENP-E dimers in the tip-tracking complexes, showing that a single FL CENP-E dimer, which contains two GFP fluorophores, can track MT tips (n=42 from 3 independent experiments). (**f**) MT velocities and catastrophe frequency in the presence or not of the tip-tracking FL CENP-E complexes (containing 1-2 dimers); Mean±SEM, n=26 shortening MTs in each group and n=28 growing MTs in each group. Tip-tracking by small CENP-E complexes does not significantly affect the rate of growth (p=0.22) and shortening (p=0.89), based on the unpaired t-test. The catastrophe frequency (Mean±SEM) was determined from n=6 independent experiments. MT catastrophe frequency with and without the tracking FL CENP-E molecules is not significantly different (p=0.6, Mann-Whitney U-test).

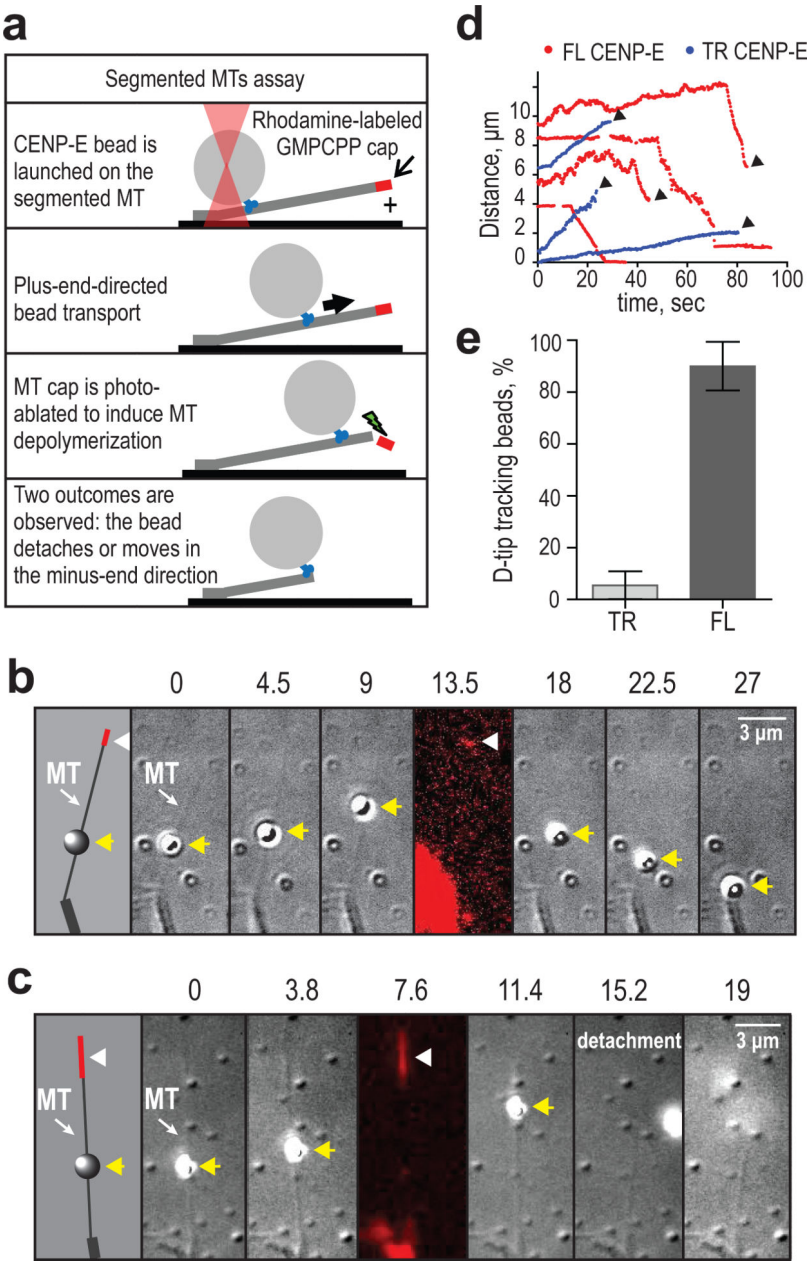

Figure 4. Motion of bead cargo in association with MT disassembly

(a) Schematics of the segmented MT assay in vitro using bead cargo. **(b, c)** A cartoon and still images from segmented MT assay with FL (panels b) and TR CENP-E-coated beads (panels c). Bead (yellow arrowhead) was placed on a capped MT grown from a coverslip-attached axoneme, as drawn in the left panel. Fluorescently-labeled cap (white arrowhead) was photo-ablated via the Rhodamine excitation (red color). All other images were recorded with DIC illumination. Numbers above panels are seconds from the start of bead's walking. **(d)** Sample motions of the CENP-E-coated beads. Distance is from the minus MT end. Arrowheads indicate bead detachment from the MT. FL CENP-E-coated beads sometimes remained attached even after MT has stopped shortening. **(e)** Tip-tracking frequency of FL

(n=10) and TR CENP-E coated beads (n=18). Error bars are SEM estimated by bootstrapping (n=1,000 samples).

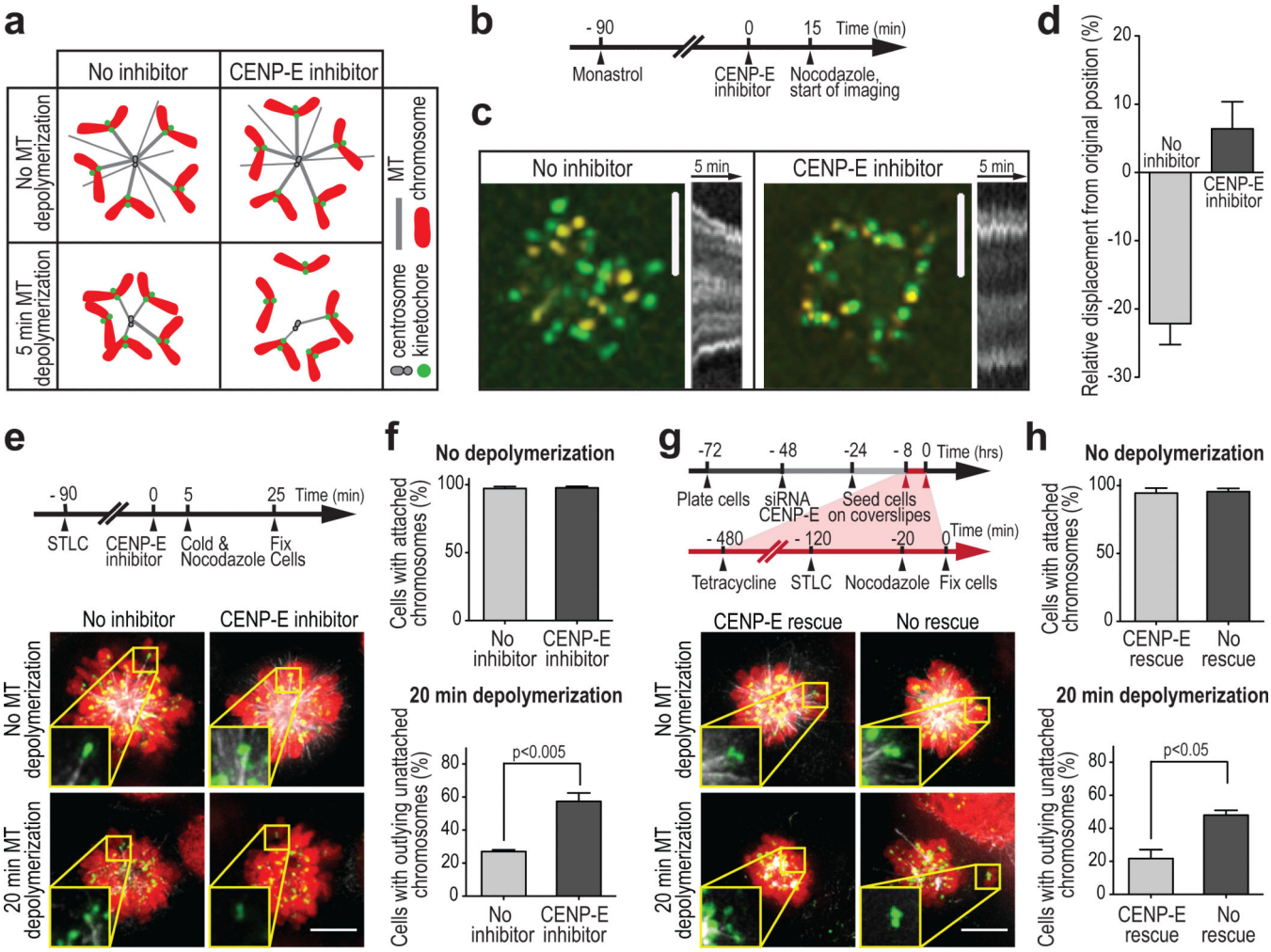

Figure 5. Investigation of CENP-E's role in depolymerization-driven chromosome motions in vivo

(a) Schematics of the MT destabilization assay to study chromosome transport by shortening MTs and summary of the main results. **(b)** Timeline of the MT destabilization assay with monopolar spindles in HeLa cells expressing Mis12-GFP (live imaging). **(c)** Two frames of Mis12-GFP kinetochore markers from a time-lapse series for each indicated condition were overlaid to reveal a shift in kinetochore position following the nocodazole-induced MT depolymerization (kinetochores in green - prior to nocodazole treatment; in yellow - 5 min after. Grayscale images are the corresponding kymographs (Video S10); scans were made across chromosome rosettes. Bar 5μm. **(d)** Relative change in the position of kinetochores prior and 5 min after nocodazole addition (Mean ± SEM, n=10 cells for each group examined in 4 independent experiments; see Eq. 1 in Materials and Methods). One way ANOVA test indicates $p<0.001$, so the means are statistically different. **(e)** Timeline of MT destabilization assay in HeLa cells and representative images (from n=3 independent experiments). Insets show enlarged images of the kinetochores (green) and MTs (white) at the periphery of the chromosome sphere; note the absence of kinetochore-attached MTs on the lower right image. Red color shows DNA (Fig. S7a). Bar 5 μm. **(f)** Proportion of HeLa cells with MT-attached chromosomes before MT depolymerization (top graph) and cells

with “outlying unattached chromosomes” after MT depolymerization (bottom graph); chromosomes at the periphery of the chromosome sphere with no attached cold-stable MT fibers were scored as “outlying unattached chromosomes”. Mean ± SEM, n=3 independent experiments; p was determined from two-tailed unpaired t test; total of 87 cells for the inhibitor condition and 89 for control were examined. **(g)** Timeline of MT destabilization assay with DLD-1 cells and representative images (from n=3 independent experiments), see legend to panel e for details. **(h)** Quantification of kinetochore-MT attachment in DLD-1 cells, see legend to panel f for details; Mean ± SEM, n=3 independent experiments. In total 78 cells were analyzed with and 75 with no CENP-E rescue.

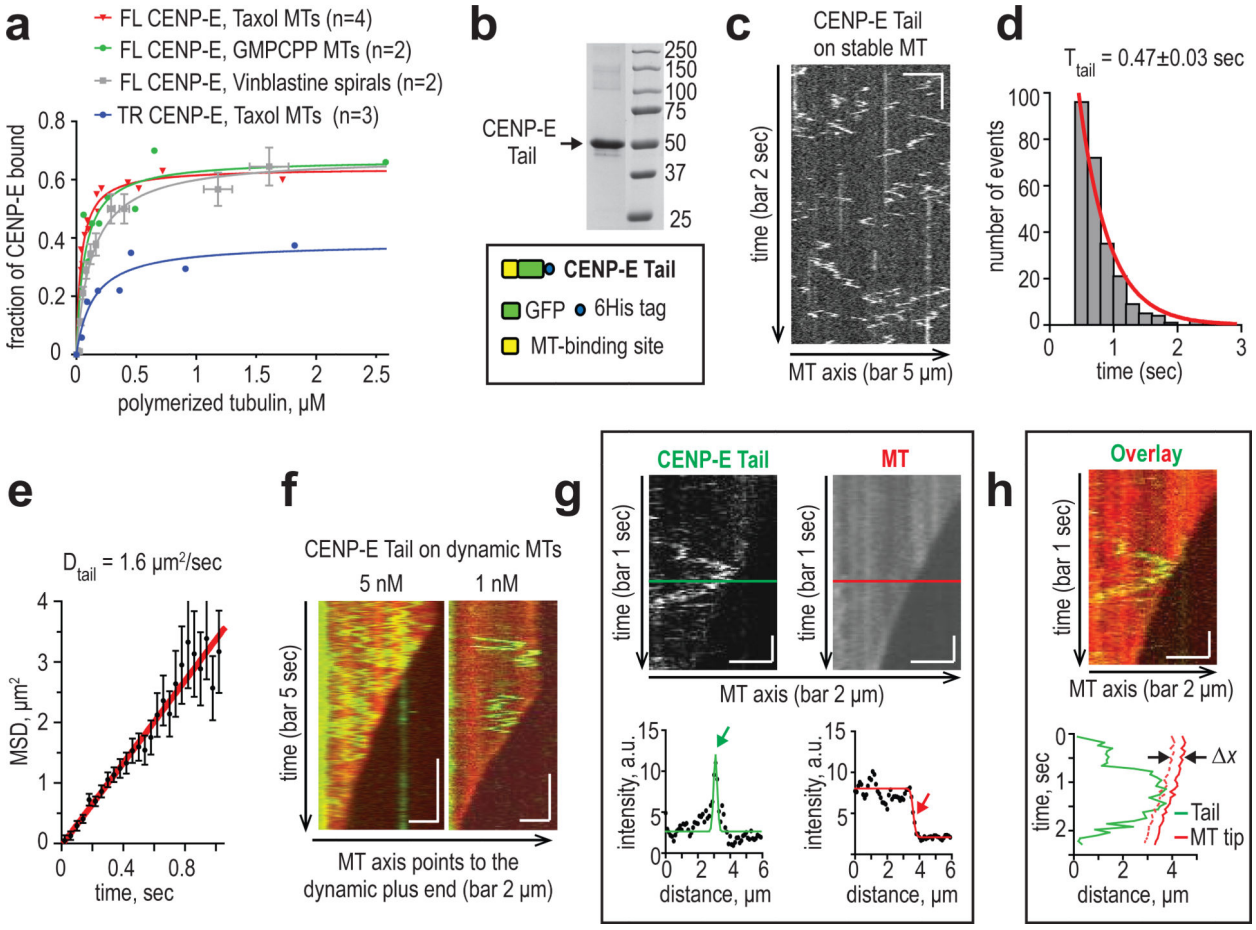

Figure 6. Analysis of possible mechanisms of CENP-E tip-tracking

(**a**) Binding affinity of FL CENP-E to different tubulin structures. Affinity to the GDP-containing MT walls was measured with Taxol-stabilized MTs; to the growing MT ends with GMPCPP-containing MTs, in which tubulin structure is likely to be similar to that at the polymerizing tips. To mimic curved protofilaments, which are normally seen at the shortening MT ends, we used tubulin spirals formed by polymerization in the presence of vinblastine. Points are from individual measurements for a given tubulin concentration; data were collected in n independent experiments, as indicated for each curve. Error bars for experiments with vinblastine spirals (Mean ± SEM) take into account that on average only 82% of spirals pelleted, while other tubulin structures pelleted completely. **(b)** SDS PAGE of purified CENP-E Tail protein containing 199 amino-acids. **(c)** Kymograph of Tail diffusion. **(d)** Histogram of residence time of Tail on MT lattice shows that the characteristic residency time for Tail in vitro is ~0.5 sec (n=378 molecules). **(e)** Mean squared displacement (MSD) for Tail vs. time with a linear fit (red). Bars are SEM, n=433 molecules. **(f)** Kymographs of Tails (green) on dynamic MTs (red); there is no processive association with growing or shortening MT ends. **(g, h)** Quantitative analysis of Tail behavior at MT tips. Upper kymographs on **(g)** show a Tail molecule diffusing near the shortening end. The intensity profiles along the colored lines are shown below. Tail and MT tip coordinates were determined as described in Materials and Methods. **(h)** Two-color

overlay (top panel) for the same molecule as in **g** but with reconstructed trajectories (bottom graph). Broken red line marks the distance from the MT tip Δ*x*, which the Tail can travel during 60 msec, the acquisition time for one frame. Tail was scored as “reflected” from the tip when the Tail was found between two red lines and then moved away from the tip, as shown in this example.

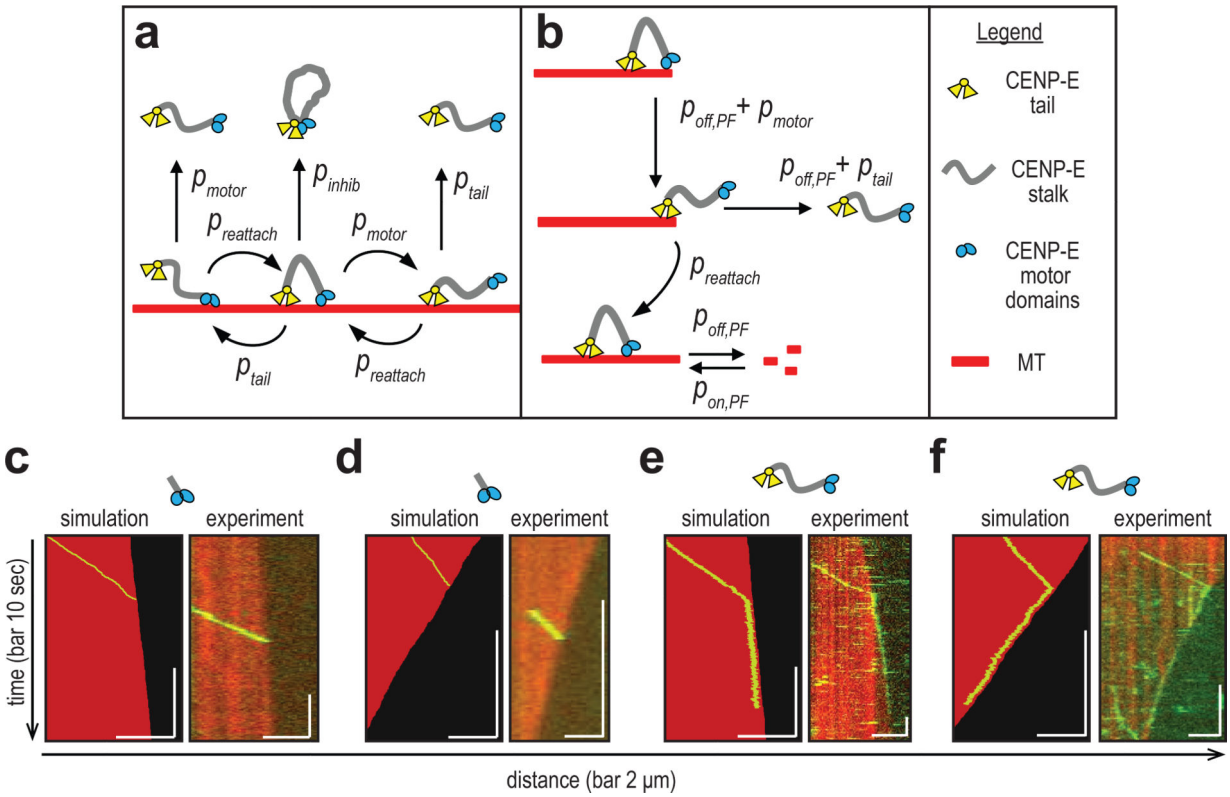

Figure 7. Mathematical model of CENP-E motility and comparison with the results of in vitro study

(a, b) Kinetic schemes for the in silico CENP-E motility on the MT lattice (panel a) and the MT tip (panel b). Arrows depict the transitions between different kinetic states with the rate constants *p* listed in Table S3. See legend on the right for more details. **(c-f)** Simulated motility kymographs of TR and FL CENP-E in silico and the representative kymographs for respective motions in vitro. Green lines in simulated kymographs are the CENP-E coordinates, red boundary is based on the coordinates of MT ends. Model predictions correspond well with experimental observations, see Supplementary Note for more details.

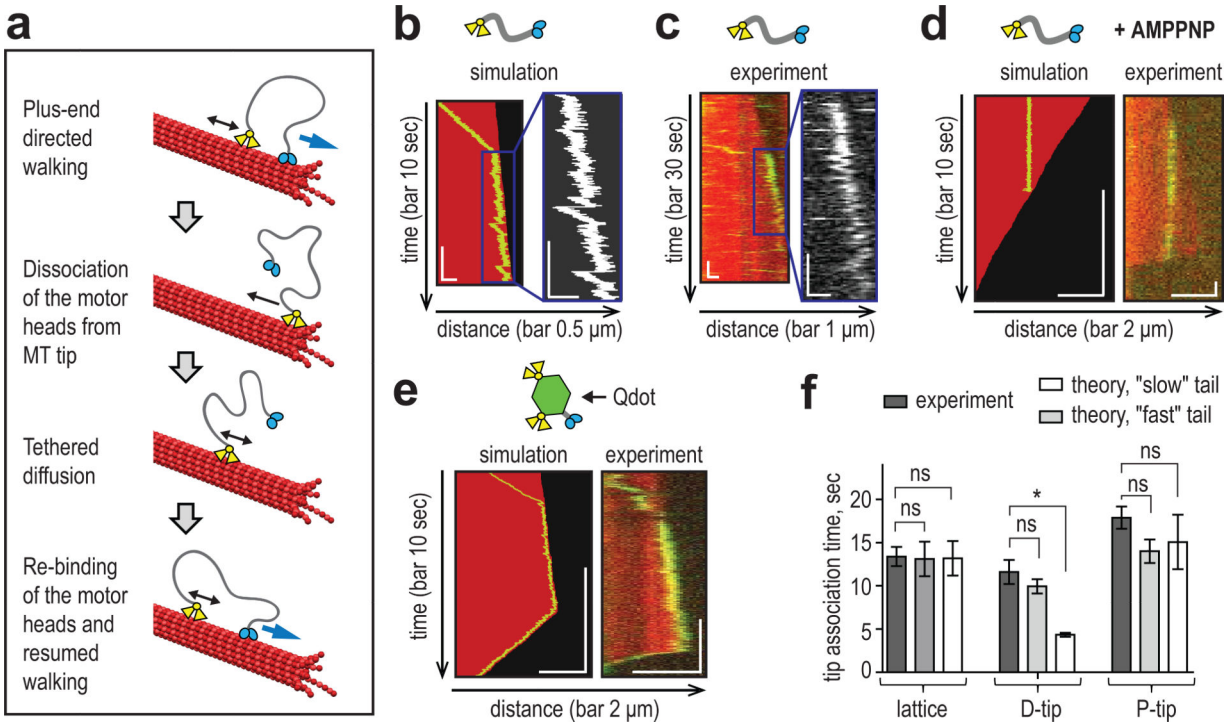

Figure 8. "Tethered motor" mechanism for processive and bi-directional MT tip-tracking and the testing of its predictions

(**a**) Diagram for the "tethered motor" mechanism of bi-directional tip-tracking. Blue arrow shows unidirectional motor's walking, black arrows - tails' diffusion and "reflection" from the tip. **(b)** Theoretical and **(c)** experimental kymographs of the FL CENP-E tracking of the growing tip. Insets show zooms of the ragged CENP-E tracings, with occasional large, minus-end-directed excursions. Such excursions are explained in the model by the tail-mediated diffusion of the tethered-motor. **(d)** Theoretical and experimental kymographs of FL CENP-E on a shortening MT in 2mM AMPPNP, which blocks motor's walking. Model predicts that the stalled motor should detach when the wave of MT depolymerization reaches its attachment site, which is indeed observed in vitro. Similar results were seen with GSK-923295, as expected. **(e)** Theoretical and experimental kymographs of Qdot coated with a mixture of TR CENP-E and Tail proteins. Such dots exhibit same motile properties as the FL molecule – they walk on MT wall unidirectionally and convert into bi-directional tip-trackers at the MT end. (**f**) Mean lattice and tip-association times for single molecules of FL CENP-E in the experiment (experimental data are from Tables S1 and S2) and as obtained in simulations ("Theory"). The diffusion coefficient of the "fast" tail in silico matches that of the CENP-E Tail protein in vitro (Fig. 6e). The "slow" diffusion coefficient is as reported for the tail of Kif18A[43]. In this range, tail's diffusion has a stronger effect on tracking the depolymerizing, but not polymerizing MT ends. Mean±S.E.M., based on 50 calculations for each motor. *- $p<0.001$; ns - $p>0.05$ (unpaired t-test).